Reduction of multiple narrow-band noises from radio waves

Reduction of multiple narrow-band noises from radio waves

Akihiro HIRANO Mitsunori OZAKI Satoshi YAGITANI
Kanazawa University

ABSTRACT This paper proposes reduction of multiple narrow-band noise signals from radio signals. The multiple narrow-band noise signals are suppressed one-by-one basis by using sinusoidal signal generators and an adaptive filter. The frequencies are estimated from the amplitude spectrum. Based on the histogram of frequency differences, low-power harmonic components can be detected. Fine tuning on frequency is carried out by using the averaged power pattern of three narrow-band-filter outputs. Peak filters are introduced in order to suppress influence of wide-band signals. The performance are examined by using real measured signals.

1 Introduction

Artificial satellites are one of the most important infrastructure for communications, transportation, navigation, etc. Failures and anomalies of such satellites might cause troubles on our daily life[1]. Analyses on such failures and anomalies show that the reasons include space environments such as ions, electrons, plasmas[2].

Measurements of radio waves from space is one of the useful tools for investigation of the space environments. Analyses of radio waves derive information on charged particles in the magnetosphere. Ground-based observation can continuously capture signals with high time resolution[3]. However, recorded signals contain interferences such as narrow-band noises from power line, pulses from GPS receiver.

This paper discusses reduction of multiple narrow-band noise signals from radio waves. Section 2 describes measured signals, followed by conventional methods for narrow-band noise reduction. Section 4 proposes a noise reduction algorithm. Experimental results with a real data shows the performance of the proposed method.

2 Measurement Data

In this research, observations of very low frequency (VLF) radio waves at Athabasca, Canada[3] are used. The VLF waves have been recorded continuously for several days with a sampling frequency of 100 kHz. This measurement results in a large number of samples. Therefore, efficient signal processing is necessary.

An example of the waveform is shown in Fig. 1. It contains two types of interferences: impulsive and narrow-band noise signals. Periodic impulses in Fig. 1 come from leakage of GPS pulses. Some impulsive noise are generated from thunder.

Figure 2 depicts the spectrogram of a noisy measured signal. Three groups of rising-tone chorus from 2 to 3.5 kHz can be seen around 10, 30 and 50 seconds. Such

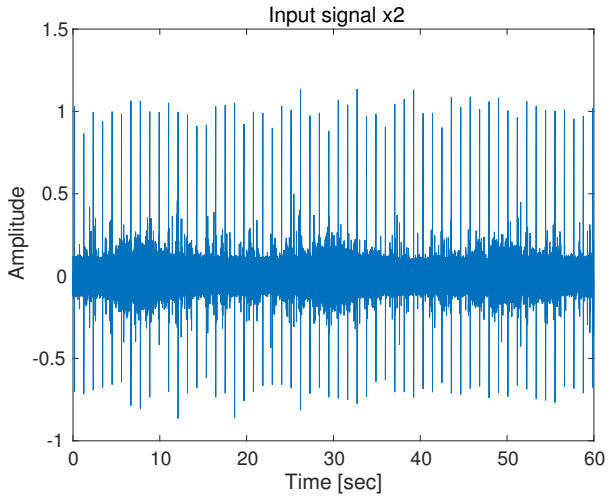

Figure 1: Waveform of noisy signal.

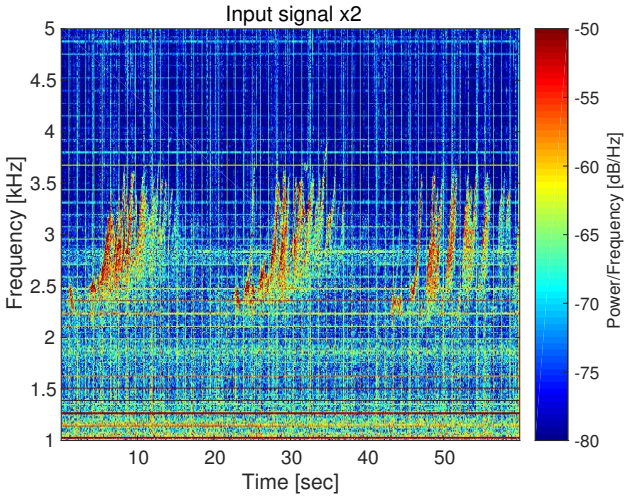

Figure 2: Spectrogram of noisy signal.

signals will be detected and used for further analysis. The horizontal lines in the spectrogram correspond to narrow-band noise signals. The main source of these signals is AC power line, which generates multiple harmonic components. The impulses look like vertical bars in the spectrogram. This work concentrate on the reduction of the narrow-band noise signals.

3 Narrow-Band Noise Reduction

There are many methods for suppressing narrow-band interference. Examples are adaptive notch filters with a parametric spectral estimation[4] and frequency-domain speech-enhancement based on spectral subtraction (SS)[5]. Frequency-domain approaches are also applied for radio-wave data[6]. However, signal distortion

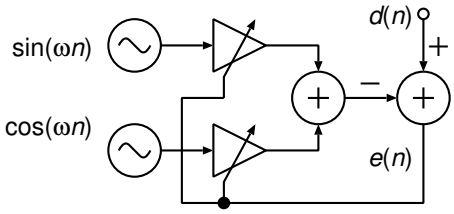

Figure 3: Sinusoidal noise reduction.

caused by noise removal is a drawback. Therefore, this work uses time-domain adaptive filtering[7].

A single sinusoidal signal case is shown in Fig. 3. It consists of two signal generators for sin and cos signals. The amplitude and the phase are controlled by a two-tap adaptive filters with $s(n)$ and $c(n)$:

$$\hat{d}(n) = s(n)\sin(\omega n) + c(n)\cos(\omega n) \tag{1}$$

$$e(n) = e(n) - \hat{d}(n). \tag{2}$$

Assuming the LMS (Least-Mean-Square) algorithm[7], the coefficients are updated by

$$s(n+1) = s(n) + \mu e(n)\sin(\omega_i n) \tag{3}$$

$$c(n+1) = c(n) + \mu e(n)\cos(\omega_i n) \tag{4}$$

where μ is a step-size parameter which controls the convergence.

A drawback of this approach would be a frequency estimation of narrow-band signal especially for a multiple unknown signal case. For such an estimation, high-resolution estimation algorithms such as the multiple signal classification (MUSIC) algorithm[8] and Estimation of Signal Parameters Via Rotational Invariance Techniques (ESPRIT)[9] are available. In this work, a simple FFT (Fast Fourier Transform)-based method is used because comparison of the computation time for some algorithms including the MUSIC [10] shows that FFT-based algorithm is very light-weight.

4 Proposed Method

4.1 Overview

The proposed noise reduction consists of multiple stages shown below.

- Frequency estimation
- Frequency interpolation
- Noise reduction

After detecting the peaks in the frequency domain, low-power peaks which are not detected in the previous stage are estimated. By using a list of frequencies, the narrow-band signals are cancelled one-by-one basis.

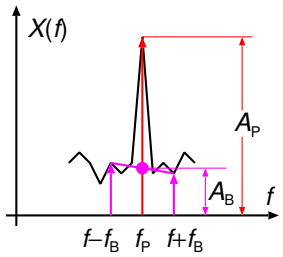

Figure 4: Peak detection in frequency domain.

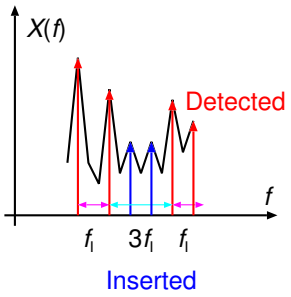

Figure 5: Frequency interpolation.

4.2 Frequency Estimation

Although many algorithms such as MUSIC are available, an FFT-based algorithm is used for simplicity. An averaged amplitude spectrum $X(f)$ over multiple segments is used.

Figure 4 shows the peak-detection method. If $X(f)$ is a local maxima at the frequency f_P, the peak amplitude A_P and the estimated background amplitude A_B are compared. These amplitude are calculated by

$$A_P = X(f_P) \tag{5}$$

$$A_B = \frac{X(f_P - f_B) + X(f_P + f_B)}{2}. \tag{6}$$

where f_B is a frequency width wider than narrow-band peaks. The peak at f_P will be detected as a narrow-band noise signal if

$$A_P > a_{Th} A_B \tag{7}$$

is satisfied where a_{Th} is a constant for amplitude ratio. This process will be repeated over pre-defined frequency region.

4.3 Frequency Interpolation

Sometimes, low-power narrow-band noise signals cannot be detected. By assuming harmonic signals, low-power peaks can be recovered. As the frequency interval, the mode of the frequency interval between neighboring peaks from the histogram is used. If the interval between neighboring peaks is almost equal to the multiple of the mode, new peaks will be inserted.

Figure 5 demonstrates a simple example. The interval is almost $3f_I$. Therefore, two peaks drawn by blue are inserted.

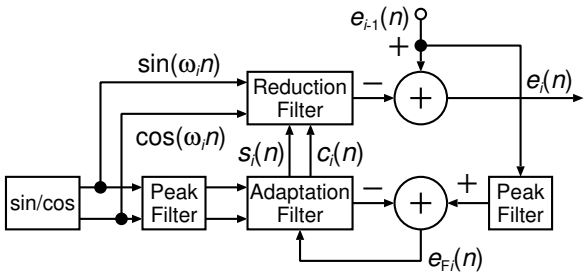

Figure 6: Proposed noise reduction.

4.4 Noise Reduction

The block diagram of the proposed noise reduction for one narrow-band signal is shown in Fig. 6. One sinusoidal noise will be cancelled by

$$\hat{d}_i(n) = s_i(n)\sin(\omega_i n) + c_i(n)\cos(\omega_i n) \tag{8}$$

$$e_i(n) = e_{i-1}(n) - \hat{d}_i(n) \tag{9}$$

$$e_0(n) = x(n). \tag{10}$$

This process will be repeated for all the detected sinusoids.

In order to suppress the influence of the wide-band signals or the impulses, peak filters are introduced. Figure 6 shows the structure of the noise reduction system for one narrow-band noise signals. The adaptation filter updates the filter coefficients $s_i(n)$ and $c_i(n)$. The reduction filter uses the coefficients from the adaptation filter.

As the peak filters, 2nd-order IIR (Infinite Impulse Response) filter defined by

$$H(z) = \frac{g(1-z^{-2})}{1-2g\cos(\pi f_0) + (2g-1)z^{-2}} \tag{11}$$

are used, where f_0 is the normalized central frequency. The gain parameter g is calculated by

$$g = \frac{1}{1+\beta} \tag{12}$$

$$\beta = \frac{\pi f_W}{\sqrt{1-(\pi f_W)^2}}\tan(\frac{\pi f_W}{2}). \tag{13}$$

The normalized band-width parameter f_W specifies the frequency where the filter gain is -3dB smaller than the peak.

The adaptation filter updates the filter coefficients $s_i(n)$ and $c_i(n)4$ by using the filtered versions of the input signals and the desired signal. The adaptation is carried out by

$$\hat{d}_{Fi}(n) = s_i(n)\sin_F(\omega_i n) + c_i(n)\cos_F(\omega_i n) \tag{14}$$

$$e_{Fi}(n) = e_{Fi-1}(n) - \hat{d}_{Fi}(n) \tag{15}$$

$$s_i(n+1) = s_i(n) + \mu e_{Fi}(n)\sin_F(\omega_i n) \tag{16}$$

$$c_i(n+1) = c_i(n) + \mu e_{Fi}(n)\cos_F(\omega_i n). \tag{17}$$

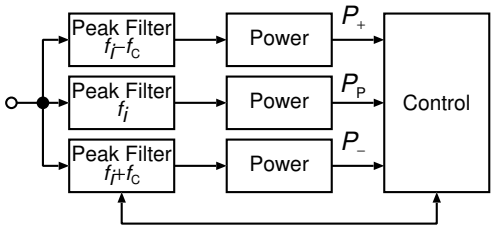

Figure 7: Structure of frequency controller.

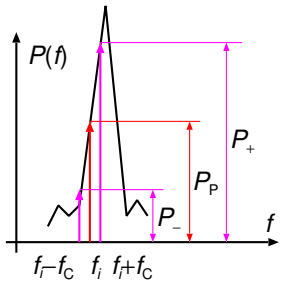

Figure 8: Principle of frequency control.

The filtered input signals $\sin_F(\omega_i n)$ and $\cos_F(\omega_i n)$ are generated by filtering the sinusoidal functions $\sin(\omega_i n)$ and $\cos(\omega_i n)$ with the IIR peak filters. Similarly, $d_{Fi}(n)$ is the filtered version of the error $d_i(n)$.

4.5 Frequency Fine-Tuning

The frequency f_i of the i-th sinusoidal signal is controlled by using peak-filters and power calculators. Figure 7 shows the block diagram of the frequency controller. The signal powers P_P, P_- and P_+ of the peak filter outputs at the frequencies f_i, $f_i - f_c$ and $f_i + f_C$ are compared by the controller. f_C is the frequency-control step-size. If

$$P_- < P_P < P_+ \tag{18}$$

is satisfied as shown in Fig. 8, the frequency f_i is modified by

$$f_i = f_i + f_C \tag{19}$$

and vice versa. As the peak filters, 2nd-order IIR filters in (11) are used.

(20)

5 Experimental Results

The performance of the proposed method has been examined by using measured signal shown in Figs. 1 and 2. For frequency estimation, 16,384-point FFT and averaging over 20 frames are used. The power-ratio parameter $a_T h$ is chosen as 1.8 by experiments. Figure 9 shows the averaged amplitude spectrum of noisy signal with detected peaks marked by red asterisks. The proposed peak detection algorithm cannot detect small peaks around 2kHz and 3kHz because their amplitude are not so higher than other signals.

The detected peaks after the interpolation stage are shown by Fig. 9. The small peaks around 2kHz and 3kHz are successfully detected.

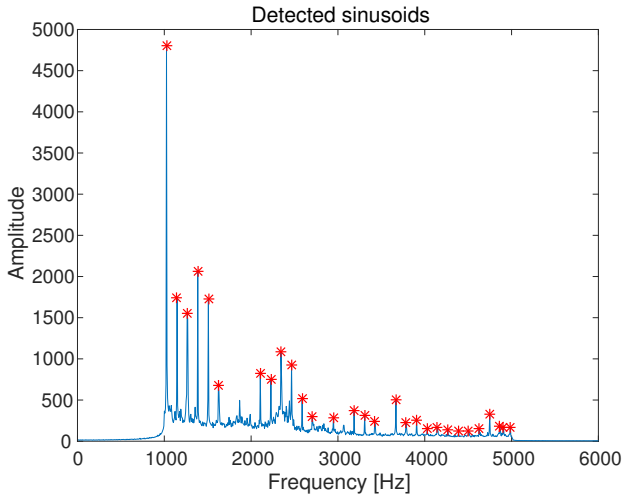

Figure 9: Detected narrow-band noises.

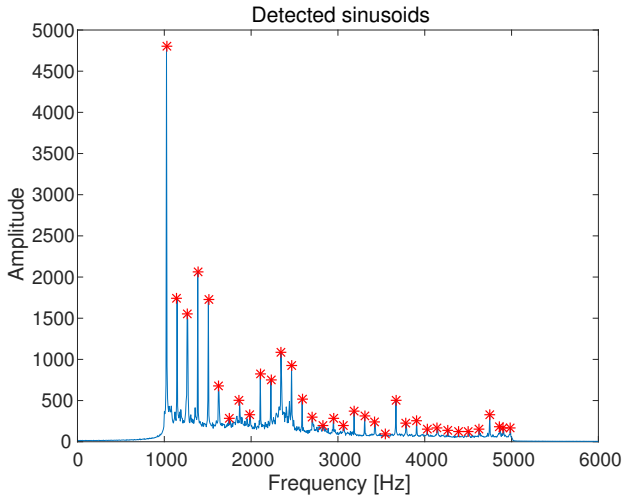

Figure 10: Narrow-band noises after interpolation.

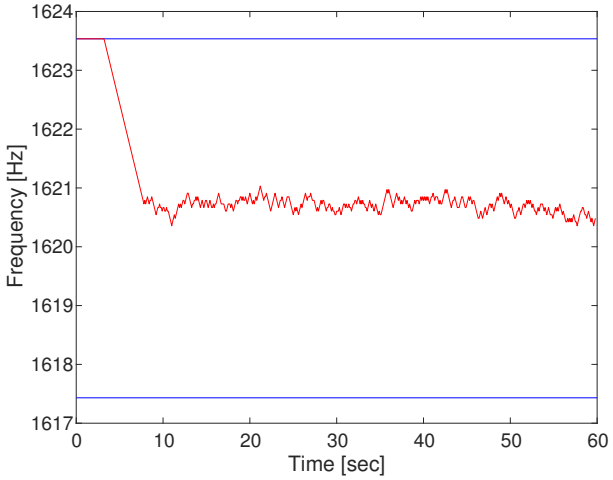

Figure 11: Estimated frequency.

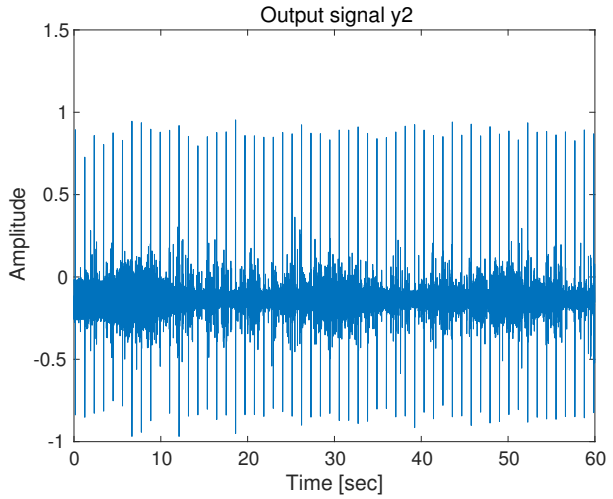

Figure 12: Power spectrum of output signal.

Figure 11 depicts estimated frequency for 6-th sinusoid. Two horizontal lines correspond to frequencies by the FFT. The frequency-control step-size f_C is chosen as $0.01 * f_S/N_{FFT}$ where f_S is the sampling frequency (100kHz), N_{FFT} is the FFT windows size (16,384). The narrow-band noise detection and their frequency estimation requires almost three seconds of the input signal. The fine tuning starts just after detection stage. The estimated frequency converges at 8 seconds. After convergence, a long-term variations can be seen.

The noise-reduced waveform and its spectrogram are shown by Figs. 12 and 13, respectively. The adaptation step-size μ is 0.001. Almost all narrow-band noise signals are successfully suppressed. No distortion can be found. Figure 14 demonstrates the effect of the interpolation stage. Comparing Figs. 13 and 14 clearly shows cancellation of narrow-band noise signals at 2kHz and 3kHz.

Figure 15 shows the spectrogram by the standard sinusoidal signal cancellation shown by Fig. 3 Multiple horizontal lines can be seen. The standard canceller fails to suppress some narrow-band noise signals.

The main reason of such residual noises can be examined by introducing the frequency fine-tuning. The spectrogram by the standard cancellers with the frequency fine-tuning is shown in Fig. 16. The step-size μ is 0.0001, which is ten-times smaller than the proposed method. By using the frequency fine-tuning, the cancellation performance is greatly improved. Although noises can be suppressed with $\mu = 0.001$, the degradation of the signal quality by over-cancellation are seen.

The effect of the peak filters can be examined by comparing Figs. 13 and 16. Although the difference is not so large, some over-cancellation at the impulsive noise (vertical bars) can be found in Fig. 16 without the peak filters. Another benefit of the peak filters is easier step-seize selection than that without the peak filters. By using the peak filters, a larger step-size can be used without spectrum degradation. Even the step-size of $\mu = 0.2$ results in a similar quality as shown in Fig. 16.

6 Conclusions

A method for the reduction of multiple narrow-band signals has been proposed. It consists of frequency estimation, frequency interpolation, and reduction stages.

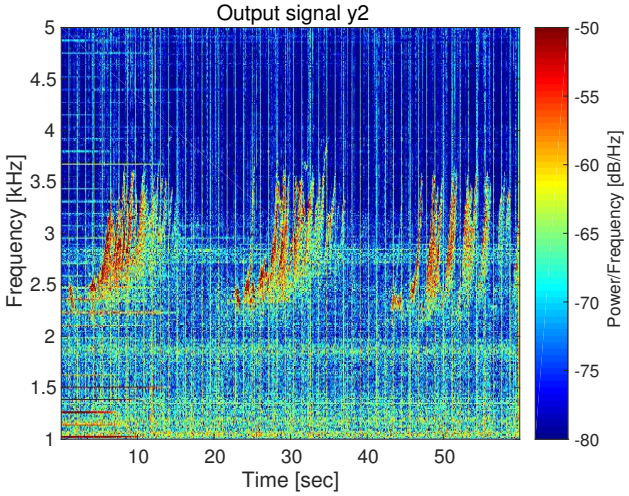

Figure 13: Power spectrum of output signal.

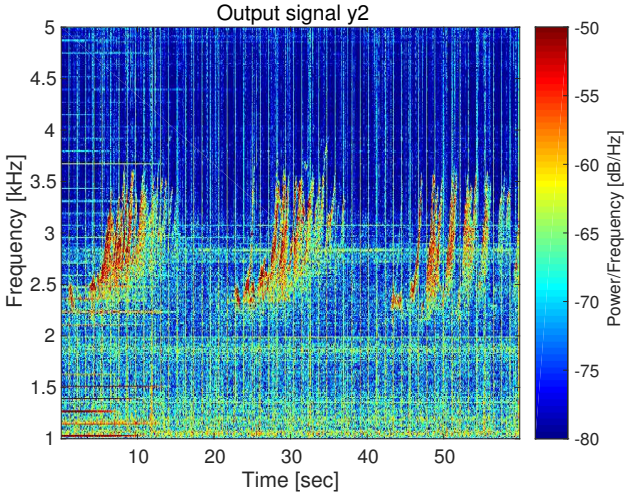

Figure 14: Power spectrum without interpolation.

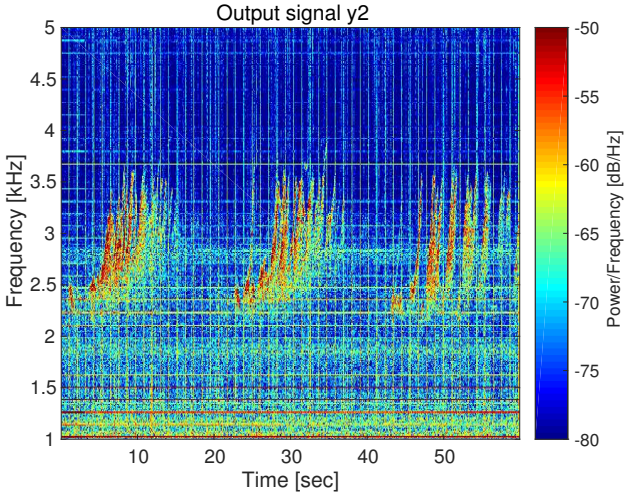

Figure 15: Power spectrum by standard canceller.

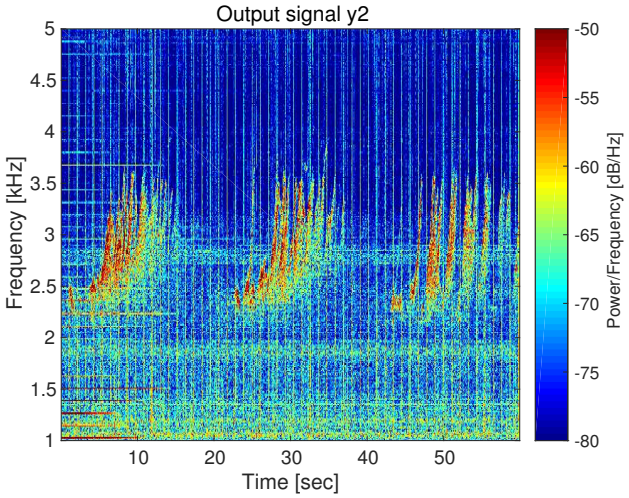

Figure 16: Power spectrum without peak filters.

Low-power harmonic components can be detected by the frequency-interpolation stage. Fine tuning of the estimated frequency within the reduction stage improves the reduction performance. The introduction of the peak filters improves output signal quality and also makes step-size selection easier.

7 Acknowledgments

This research is supported as a part of the SAKIGAKE project, Kanazawa University.

References

[1] R. D. Leach and M. B. Alexander, "Failures and anomalies attributed to spacecraft charging," *NASA Reference Publication*, , no. 1375, Aug. 1995.

[2] H. S. Choi, J. Lee, K. S. Cho, Y. S. Kwak, I. H. Cho, Y. D. Park, Y. H. Kim, D. N. Baker, G. D. Reeves, and D. K. Lee, "Analysis of GEO spacecraft anomalies: Space weather relationships," *Space Weather*, vol. 9, no. 6, Jun. 2011.

[3] K. Shiokawa, Y. Yokoyama, A. Ieda Y. Miyoshi, R. Nomura, S. Lee, N. Sunagawa, Y. Miyashita, M. Ozaki, K. Ishizaka, S. Yagitani, R. Kataoka, F. Tsuchiya, I. Schofield, and M. Connors, "Ground-based elf/vlf chorus observations at subauroral latitudesvlf-chain campaign," *Journal of Geographical Research*, vol. 119, no. 9, pp. 7363–7379, Sep. 2014.

[4] A. Nehorai, "A minimal parameter adaptive notch filter with constrained poles and zeros," *IEEE Trans. ASSP*, vol. ASSP-33, no. 4, pp. 983–995, Aug. 1985.

[5] Y.Ephraim and D.Malah, "Speech enhancement using minimum mean-square error shorttime spectral amplitude estimator," *IEEE Trans ASSP*, vol. ASSP-32, no. 6, pp. 1109–1121, Dec. 1984.

[6] T. Dejima, M. Ozaki, S. Yagitani, K. Shiokawa, Y. Miyoshi, M. Miyoshi, A. Hirano, and M. Connors, "Study on the noise reduction technique for VLF emissions by audio signal processing (in japanese)," *Proc. of Japan Geoscience Union Meeting*, pp. PEM18–P13, May 2016.

[7] B. Widrow and S. D. Stearns, "Adaptive noise canceling: Principles and applications," *Proc. of IEEE*, vol. 63, no. 12, pp. 1692–1716, Dec 1975.

[8] R. Schmidt, "Multiple emitter location and signal parameter estimation," *IEEE Trans. AP*, vol. 34, no. 3, pp. 276–280, Mar. 1986.

[9] R. Roy and T. Kailath, "ESPRIT-estimation of signal parameters via rotational invariance techniques," *IEEE Trans. ASSP*, vol. ASSP-37, no. 7, pp. 984–995, Jul. 1989.

[10] A. Ahmad, F. S. Schlindwein, and G. A. Ng, "Comparison of computation time for estimation of dominant frequency of atrial electrograms: Fast fourier transform, blackman tukey, autoregressive and multiple signal classification," *J. Biomedical Science and Engineering*, pp. 843–847, Mar. 2010.